Lung Cancer 135 (2019) 40–46

Contents lists available at ScienceDirect

Lung Cancer

journal homepage: www.elsevier.com/locate/lungcan

Toward improving prognosis prediction in patients undergoing small lung adenocarcinoma resection: Radiological and pathological assessment of diversity and intratumor heterogeneity

Satoshi Koezuka[a], Tetuo Mikami[b], Naobumi Tochigi[c], Atsushi Sano[a], Yoko Azuma[a], Takashi Makino[a], Hajime Otsuka[a], Keiko Matsumoto[d], Nobuyuki Shiraga[d], Akira Iyoda[a,*]

[a] Division of Chest Surgery, Toho University School of Medicine, 6-11-1 Omori-nishi, Ota-ku, Tokyo, 143-8541, Japan
[b] Department of Pathology, Toho University School of Medicine, 5-21-16 Omori-nishi, Ota-ku, Tokyo, 143-8540, Japan
[c] Department of Surgical Pathology, Toho University School of Medicine, 6-11-1 Omori-nishi, Ota-ku, Tokyo, 143-8541, Japan
[d] Department of Radiology, Toho University School of Medicine, 6-11-1 Omori-nishi, Ota-ku, Tokyo, 143-8541, Japan

ARTICLE INFO

Keywords:
Adenocarcinoma
Ground-glass opacity
Diversity
Intratumor heterogeneity
Programmed cell death ligand 1 expression

ABSTRACT

Objectives: Prediction of prognosis based on the ground-glass opacity (GGO) ratio for small (≤2 cm) lung adenocarcinomas is not completely accurate. The aim of this study was to clarify the diversity of small adenocarcinomas and to identify ways to more accurately predict prognosis.

Materials and methods: We retrospectively reviewed 62 patients (64 lesions) that underwent lobectomy for small (≤2 cm) lung adenocarcinoma. Proportions of histological components were measured and the presence of tumor spread through air spaces (STAS) was assessed. The correlations between GGO and histological components were examined. Furthermore, histological components of pure GGO lesions were analyzed using CT values. The intratumor heterogeneity of programmed death ligand 1 (PD-L1) expression was analyzed in 40 lesions. Furthermore, the relationship between CT/histological findings and prognoses was analyzed.

Results: In 13 pure GGO lesions, 7 (53.8%) lesions contained invasive components such as papillary, acinar, solid, and colloid. Tumor spread through air spaces (STAS) was also found in pure GGO lesions. Pure GGO lesions containing invasive components ($p = 0.002$) and STAS-positive lesions ($p = 0.011$) demonstrated strongly higher CT value. Differences in expression of PD-L1 among histological subtypes were observed in four of six (66.7%) PD-L1 positive lesions. Patients with papillary component, positivity for STAS, or CT value ≥ -140.6 Hounsfield units (HU) had significant poorer prognoses than patients without those in disease-free survival analyses ($p = 0.007$, $p = 0.048$, $p = 0.012$). Patients with the CT value < -383.4 HU and GGO ≥ 50% did not have recurrence.

Conclusions: Invasive component and STAS can be present even in small GGO lesions, and patients with papillary components or STAS showed significantly poorer prognoses. STAS-positive lesions were strongly associated with a high CT value, and combined use of GGO ratio and CT value may be able to predict recurrences of lung cancer more accurately.

1. Introduction

Lung cancer is the leading cause of cancer-related death and third most common cancer in Japan [1]. Lung adenocarcinoma is the most common histological type of lung cancer [2]. Adenocarcinomas shows diversity across both the radiologic and pathologic spectrums. Additionally, the internal structure of adenocarcinomas is heterogeneous. Radiologically, adenocarcinoma often consists of various ratios of ground-glass opacity (GGO) and solid components. GGO is defined as an opacity that does not obscure the underlying structures or vasculature on high-resolution computed tomography (CT) [3], whereas solid components are defined by an increase in attenuation

Abbreviations: DFS, disease-free survival; GGO, ground-glass opacity; HU, hounsfield units; IHC, immunohistochemistry; PD-L1, programmed death ligand 1; STAS, tumor spread through air spaces

* Corresponding author at: Division of Chest Surgery, Department of Surgery, Toho University School of Medicine, 6-11-1 Omori-nishi, Ota-ku, Tokyo, 1438541, Japan.
E-mail address: aiyoda@med.toho-u.ac.jp (A. Iyoda).

https://doi.org/10.1016/j.lungcan.2019.06.023
Received 15 March 2019; Received in revised form 22 May 2019; Accepted 24 June 2019

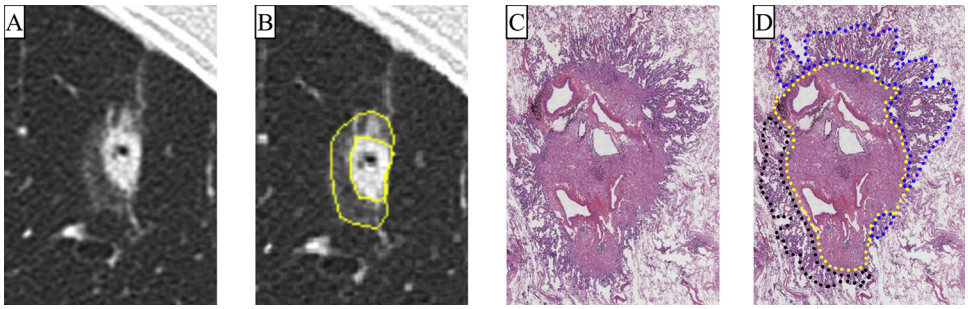

Fig. 1. (A and B) Measurement of GGO proportion. Axial CT image showing a part solid lesion (A). The whole lesion and solid component were manually outlined and areas were measured using the texture analysis software ImageJ (B). Using these values, the proportion of GGO was calculated.
(C and D) Measurement of the histological component proportion. This part solid lesion was revealed to be a papillary predominant adenocarcinoma (including fibrosis, lepidic, and papillary components) (C). Fibrosis (marked by yellow dots), lepidic components (marked by black dots), and papillary components (marked by blue dots) were manually outlined on a digitized image of the histology slide and the areas were measured using ImageJ (D). Using these values, the proportion of each component was calculated.

that obscures the underlying vascular markings. Pathologically, adenocarcinoma consists of multiple components and is divided into subtypes according to the predominant pattern [4]. In general, lepidic components, which commonly exist during early phases, correspond to GGO on a chest CT [5]. A high proportion of GGO is considered to be a favorable prognosis indicator.

In recent years, the incidence of small GGO lesions has increased due to the widespread use of high-resolution CT. Surgical resection is the only curative therapy for early-stage lung cancer. The standard surgical procedure for lung cancer is lobectomy with lymph node dissection. Sometimes, limited resection is conducted for peripheral, small lung cancers [6,7]. Several trials have explored limited resection based on the proportion of GGO. Although the prediction of postoperative prognosis is currently based on the proportion of GGO, the accuracy is not fully satisfactory. In clinical practice, even for early-stage adenocarcinomas that were preoperatively considered to be associated with a good prognosis, such as those with a high proportion of GGO or small lesions, recurrence and postoperative nodal metastasis sometimes occur.

The diversity of adenocarcinoma characteristics may make preoperative prediction of prognosis difficult. A non-lepidic, invasive component is sometimes present on postoperative histology in pure GGO lesions [8–13]. In addition, tumor spread through air spaces (STAS) was newly described as a pattern of invasion and novel poor prognostic factor in the 2015 WHO classification [14]. Which patients will benefit from limited resection presently remains a subject of research and debate. Elucidation of adenocarcinoma diversity may allow more accurate prognostic prediction and improve treatment outcomes.

The objective of the present study is to clarify the reasons that some lesions with a high GGO ratio are associated with a poor prognosis by contrasting histologic findings and CT findings, and also considering the presence of STAS. In addition, we also investigate a method of predicting GGO-predominant lesions associated with a poor prognosis using CT values. Furthermore, we examine intratumor heterogeneity by programmed death ligand 1 (PD-L1) immunohistochemistry (IHC) assays. In this study, we focused on small lung adenocarcinomas with a maximal diameter of ≤ 2 cm, and evaluated their diversity.

2. Materials and methods

2.1. Patients

This retrospective study was approved by the Ethics Committee of Toho University School of Medicine (No. A18021_27085), and informed consent was obtained from all patients. Between 2008 and 2016, 64 lesions in 62 patients who underwent lobectomy for small (≤ 2 cm) lung adenocarcinomas were evaluated retrospectively. Three lesions were resected from one patient. Medical records were reviewed to investigate clinical characteristics, CT features, pathological findings, and outcomes. The diagnosis of adenocarcinoma was made according to the 2015 WHO Classification of Lung Tumors [14].

2.2. Radiological evaluation on thin-section CT

All lesions were evaluated using a 64-detector CT row scanner (Aquilion, Toshiba, Japan or Somatom Definition Flash, Siemens, Germany) with a section thickness of 1.0 mm. All scanners were equipped with automatic exposure control (AEC) systems. Target thin-section helical CT scans (1.0 mm collimation, 0.5-second gantry rotation time, 120 kVp) were obtained. All images were viewed with lung window settings (window width, 1600 Hounsfield units [HU]; window level, 1600 HU). GGO and solid components were evaluated in the slice of maximum area on the lung window by a radiologist with 17 years of experience who was unaware of clinical data and pathological findings. The definition of GGO is a hazy increase in lung attenuation that does not obscure the underlying vascular markings. Based on the presence or absence of GGO or solid components, lesions were classified as either pure GGO lesions, part solid GGO lesions, and solid lesions. Pure GGO lesions were defined as lesions without a solid component, part solid GGO lesions were defined as lesions with both GGO and solid components, and solid lesions were defined as lesions without a GGO component. The proportion of GGO was measured using ImageJ software (NIH) (Fig. 1A,B). The CT values of the GGO and solid regions were calculated by use of AZE Virtual Place (AZE Ltd, Tokyo, Japan). When two regions of different density were observed in a pure GGO lesion, the CT value of each region was calculated; the highest value among GGO and solid regions was determined to be the CT value of the lesion. The difference between CT values in pure GGO lesions with and without a non-lepidic invasive components was evaluated. The difference between CT value in lesions with and without the specific histological component was also evaluated. Prediction probability for presence of the specific histological component was analyzed using a receiver operating characteristic curve (ROC).

2.3. Histological evaluation

All specimens were inflated and fixed with formalin, and stained using hematoxylin-eosin (H-E) and Elastica van Gieson staining. All slides for each case were reviewed by two of the authors, one of whom is a pathologist, who were unaware of both clinical data and radiological findings. The histological findings were classified according to the 2015 WHO Classification of Lung Tumors. Then, the glass slides were retrieved using a vertical slide system (TOCO, Claro Inc., Hirosaki, Japan) and converted into digital files. The occupancy ratio of each component (lepidic, papillary, acinar, solid, micropapillary, pattern of variants, fibrosis, necrosis, pleural thickening, inflammation, edema, cavities, vessels, and bronchi) in the whole lesion was measured using the digital image files and ImageJ software, and recorded in 0.1% increments (Fig. 1C,D). Pleural thickening, inflammation, edema, cavities, vessels, and bronchi ≥ 1 mm in diameter were classified as 'other components.' In addition, the presence or absence of STAS was recorded. STAS was defined as tumor cells within air spaces in the lung parenchyma at a distance of at least one alveolus away from the main

tumor, and has been previously described by Kadota et al [15].

2.4. Immunostaining

PD-L1 expression was analyzed in 40 of the 64 lesions by IHC. Samples were stained using the PD-L1 IHC 22C3 pharmDx staining kit (Agilent, Santa Clara, CA). The PD-L1 expression rate and components in which PD-L1 was expressed were examined. The relationship between PD-L1 expression and histological subtype was also analyzed.

2.5. Statistical analysis

Statistical analysis was performed using SPSS software version 22.0 (SPSS Inc; Chicago, IL, USA). The Shapiro-Wilk test was used to assess the normality of the data. Spearman rank correlation coefficients were calculated between the GGO and lepidic pattern ratios. Student's *t*-test and the Mann–Whitney U test were used to compare the differences in CT value. The effect of the following factors on the disease-free survival (DFS) were evaluated: pathological stage, lymph node metastasis, each histological component, STAS, CT findings, CT value. DFS was calculated from the date of surgery to the date of recurrence or death. DFS were calculated using the Kaplan–Meier method and survival curves were compared using log-rank test. p values < 0.05 were considered to indicate statistically significant differences.

3. Results

3.1. Radiological and histological characteristics

Radiological and histological characteristics are summarized in Table 1. A total of 64 lesions in 62 patients were evaluated. Of these, three lesions occurred in one patient. CT findings revealed 13 pure GGO lesions (20.3%), 9 part solid GGO lesions (14.1%), and 42 solid lesions (65.6%). The predominant histological subtype was lepidic in 25 lesions (39.0%), papillary in 21 lesions (32.8%), acinar in 5 lesions (7.8%), solid in 9 lesions (14.1%), and other variants in 4 lesions (6.3%); all 4 variant lesions were colloid predominant adenocarcinomas. No micropapillary predominant lesions were observed. The most common histological components present in the 64 lesions were lepidic in 41 lesions (64.1%), followed by papillary in 39 lesions (60.9%), acinar in 23 lesions (35.9%), fibrosis in 21 lesions (32.8%), solid in 15 lesions (23.4%), other in 10 lesions (15.6%), colloid in 4 lesions (6.3%), micropapillary in 4 lesions (6.3%), and necrosis in 3 lesions (4.7%). Of all lesions, 78.1% had more than two components, not including the other components category (pleural thickening, inflammation, edema, cavities, vessels, and bronchi). Five, four, three, and two components were present in 1 (1.5%), 8 (12.5%), 17 (26.6%), and 24 (37.5%) tumors, respectively. STAS was observed in 18 (28.1%) lesions. Lymph node metastasis was found in 3 (4.8%) patients. The pathologic stage was 0 in 11 (17.1%) lesions, IA1 in 29 (45.3%) lesions, IA2 in 13 (20.3%) lesions, IA3 in 2 (3.1%) lesions, IB in 6 (9.4%) lesions, and IIB 3 (4.7%) lesions.

Table 1
Radiological and Histological Characteristics of 64 lesions.

Variable	n	%
CT findings		
Pure GGO	13	20.3
Part solid	9	14.1
Solid	42	65.6
Predominant histological subtypes		
Lepidic	25	39.0
Papillary	21	32.8
Acinar	5	7.8
Solid	9	14.1
Micropapillary	0	0
Variants (colloid)	4	6.3
Histological components		
Lepidic	41	64.1
Papillary	39	60.9
Acinar	23	35.9
Solid	15	23.4
Micropapillary	4	6.3
Colloid	4	6.3
Fibrosis	21	32.8
Necrosis	3	4.7
Others	10	15.6
The numbers of components except others		
5	1	1.5
4	8	12.5
3	17	26.6
2	24	37.5
1	14	21.9
STAS		
Positive	18	28.1
Negative	46	71.9

GGO, ground glass opacity; STAS, tumor spread through air space.

3.2. Correlations between GGO components on CT and histological components

Fig. 2A shows the plots of correlation between the proportion of GGO and lepidic components for all 64 lesions. The correlation coefficient between the proportion of GGO and lepidic components was 0.579 ($p < 0.001$). Histological components corresponding to the GGO component were also assessed. Fig. 2B shows the construction of histological components within the tumor for each of the 13 pure GGO lesions. A total of seven (53.8%) lesions contained non-lepidic invasive components, such as papillary, acinar, solid, and colloid components. In six lesions, > 40% of the GGO component corresponded to a non-lepidic component. Among four of six lesions, > 70% of the GGO component corresponded to a non-lepidic component. In one of these, the lesion was composed entirely of a papillary component, with no lepidic component.

3.3. Prediction of non-lepidic invasive components in pure GGO lesions

Fig. 2C compares the CT values of pure GGO lesions with and without non-lepidic invasive components. In three pure GGO lesions, the GGO density was heterogeneous. The average of the CT value in pure GGO lesions was -492.9 HU (range, -881.8 to -216.0 HU). The CT value was -355.5 ± 129.4 HU in the lesions containing non-lepidic invasive components and -653.1 ± 135.9 HU in lesions not containing non-lepidic invasive components. Lesions containing non-lepidic invasive components were strongly associated with a high CT value ($p = 0.002$).

We specifically assessed the lesions containing non-lepidic invasive components. Fig. 3 shows the radiological and histological findings of a pure GGO lesion that relapsed as multiple lung metastases 3 years after lobectomy. Fig. 3A shows a pure GGO lesion with heterogeneous density. A high concentration of GGO components was observed in the center. The CT value of the high concentration portion was -216 HU, while the CT value of the low concentration area was -414 HU (Fig. 3B). Fig. 3C shows a lepidic-predominant adenocarcinoma. A papillary component was seen at the center of the tumor, and a lepidic component was observed around the papillary component (Fig. 3D).

3.4. Association between CT findings and STAS

STAS was present in 18 of 64 (28.1%) lesions. Among these lesions, solid lesions were the most prevalent CT finding. STAS was present in 16 of 42 (38.0%) solid lesions. Although the frequency was low, STAS was present in 1 of 9 (11.1%) partly solid lesions. Moreover, STAS was also present in 1 of 13 (7.6%) pure GGO lesions, which contained no solid components.

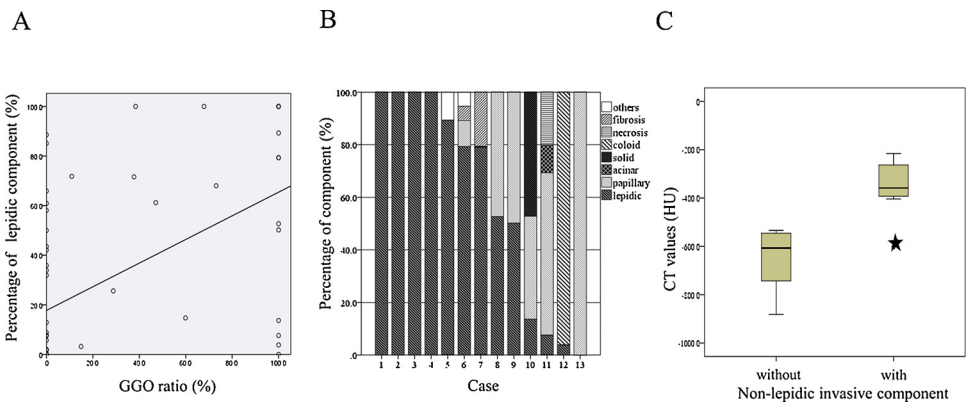

Fig. 2. (A) Correlation between the proportion of GGO and lepidic components of all 64 lesions (correlation coefficient, 0.579; $p < 0.001$).
(B) Distribution of histological component percentages of 13 pure GGO lesions.
(C) Comparison of the CT values between pure GGO lesions with and without non-lepidic, invasive components.

The CT value was -107.7 ± 112.7 HU in the STAS-positive lesions and -235.0 ± 215.7 HU in STAS-negative lesions. STAS-positive lesions showed significantly higher CT value than STAS-negative lesions did ($p = 0.011$). The optimal threshold value for presence of STAS was -140.6 HU (area under the ROC curve, 0.70; 95% CI, 0.57-0.84) with a sensitivity of 77.8% and specificity of 69.6%.

3.5. Intratumor heterogeneity of PD-L1 expression

PD-L1 was expressed in 6 of 40 (15.0%) lesions evaluated. The percentage of tumor cells that expressed PD-L1 was 5% in four lesions, 10% in one lesion, and 90% in one lesion. PD-L1 was heterogeneously expressed within the tumor in all six lesions. Fig. 4A shows a representative image of heterogeneous PD-L1 expression. Fig. 4B shows the relationship between histological subtype and PD-L1 expression for each of the six PD-L1 positive lesions. In two of these six lesions, PD-L1 expression was observed in two different subtypes. Differences in PD-L1 expression among histological subtypes were observed in four lesions. PD-L1 expression was observed in all of the solid and papillary components of six lesions, while it was not observed in any of the acinar components of six lesions.

3.6. Survival analysis

The mean follow-up time of 62 patients was 50.1 months (range, 10–124 months). The 5-year DFS rate was 82.7%. The recurrence was observed in 8 patients. On the histological factors, patients with papillary component had a significantly poorer DFS rates than patients without that (5-year DFS rate, 71.5% vs 100%, $p = 0.007$, Fig. 5A). Patients with STAS-positive lesion had a significantly poorer DFS rates than patients without that (5-year DFS rate, 67.6% vs 87.9%, $p = 0.048$, Fig. 5B). On the radiological factors, we performed survival analyses on CT value using the optimal threshold value for presence of STAS because there are no differences on CT value between positive-papillary components and negative-papillary components and we could not decide the optimal threshold value for presence of papillary components. The analysis of DFS revealed significant differences between CT value ≥ -140.6 HU and < -140.6 HU (5-year DFS rate, 69.6% vs 93.2%, $p = 0.012$, Fig. 5C). Two cases with recurrence were included in the low CT value (< -140.6 HU) lesion.

In order to assess recurrence more accurately, we used both CT values and GGO ratios to assess recurrence. Although we evaluated the prognosis divided into 2 groups based on CT value - 140.6 HU, we could not divide patients with recurrence clearly. Therefore, we used -383.4 HU, which is the lowest CT value in the STAS-positive lesion. Patients were divided into CT value < -383.4 HU and GGO ≥ 50% group and CT value ≥ -383.4 HU or GGO < 50% group. No recurrences were observed in patients with the CT value < -383.4 HU and GGO ≥ 50% group although DFS curves did not reveal significant difference between patients with the CT value < -383.4 HU and GGO ≥ 50% group and patients with CT value ≥ -383.4 HU or GGO < 50% group (5-year DFS rate, 100% vs 80.0%, $p = 0.195$, Fig. 5D).

4. Discussion

The present study aimed to provide a more accurate prediction of prognosis in small (≤2 cm) lung adenocarcinomas presenting as GGO-predominant lesions by clarifying the diversity of these adenocarcinomas. Even small (≤2 cm) lung adenocarcinomas are sometimes associated with postoperative nodal metastasis [16] and poor prognosis in clinical practice. In this study, we showed that radiological, histological, and molecular diversity exist even among small lung adenocarcinomas, GGO on CT does not always correspond to lepidic components, non-lepidic, invasive components can correspond to GGO. Moreover, CT values are useful in predicting the non-lepidic invasive components that correspond to GGO, and STAS was related with CT value and prognoses. This information is important when considering postoperative prognosis. Therefore, we think that predicting the postoperative prognosis and selecting to perform limited resection only by analyzing the proportion of GGO is problematic. One strength of the present study is its fine classification of histological components. We evaluated histological components in pure GGO lesions. Previous

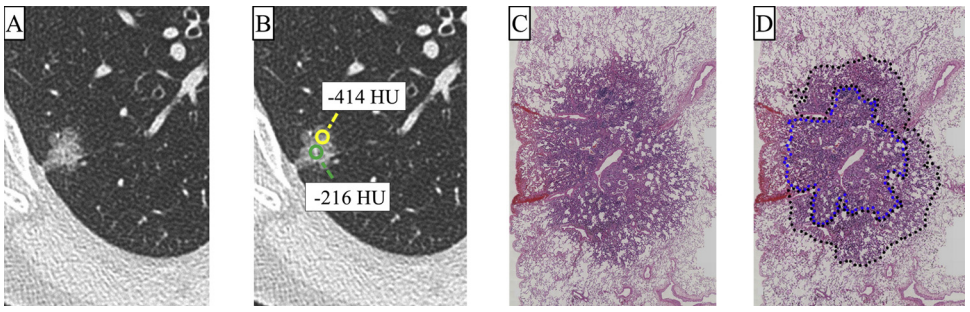

Fig. 3. A pure GGO lesion associated with a relapse of multiple lung metastases 3 years after lobectomy.
(A and B) Axial CT image shows the pure GGO lesion. The density of GGO was heterogeneous (A). The central area of the lesion was denser than the peripheral area (B).
(C and D) This pure GGO lesion revealed lepidic predominant adenocarcinoma (including lepidic and papillary components) (C). The central area of the lesion shows a papillary component (marked by blue dots), and a lepidic component (marked by black dots) is seen around the papillary component (D).

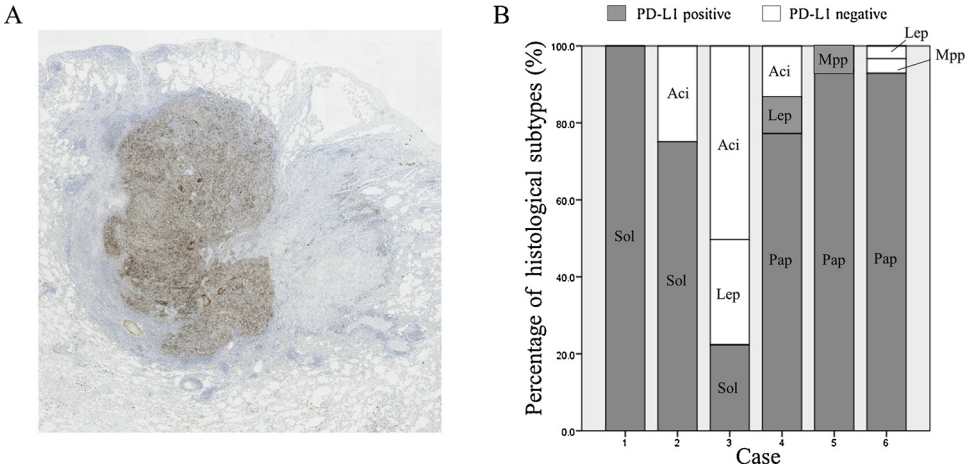

Fig. 4. Intratumor heterogeneity of PD-L1 expression.
(A) An example of a lung adenocarcinoma demonstrating heterogeneous PD-L1 expression. This lesion revealed solid predominant adenocarcinoma (including solid and acinar components). PD-L1 expression was observed in part of the solid component areas, while no PD-L1 expression was observed in acinar component areas.
(B) Association between histological subtype and PD-L1 expression in six PD-L1–positive lesions.
Lep; lepidic component, Pap; papillary component, Aci; acinar component, Sol; solid component, Mpp; micropapillary component.

studies evaluated predominant subtypes of adenocarcinoma presenting as pure GGO, and only one study evaluated histological components in pure GGO [10]. A second strength of the present study is the use of resected specimens to evaluate intratumor heterogeneity of PD-L1 expression and the histological components in which PD-L1 is expressed throughout the whole tumor. Previous studies evaluated predominant subtypes related to PD-L1 expression. Only one study evaluated the histological components of resected specimens [17].

Predicting prognosis before surgery is important for selecting the optimal surgical procedure. A prospective radiological study revealed that small lesions (≤2.0 cm in diameter) with ≤0.25 consolidation to the maximum tumor diameter can be defined as radiologically non-invasive adenocarcinoma without nodal involvement, vascular invasion, or lymphatic invasion [18]. Although sublobar resection is performed based on consolidation/tumor ratio, i.e., the GGO ratio, currently no definitive criteria exist for limited resection. Recently, Moon et al. showed that non-lepidic invasive components such as acinar and papillary components in pure GGO lesions do not influence prognosis after resection [10]. These investigators reported that invasive adenocarcinomas presenting as GGO-predominant tumors were associated with a 100% 5-year relapse-free survival rate following sublobar resection. However, in the clinical setting, small adenocarcinomas that

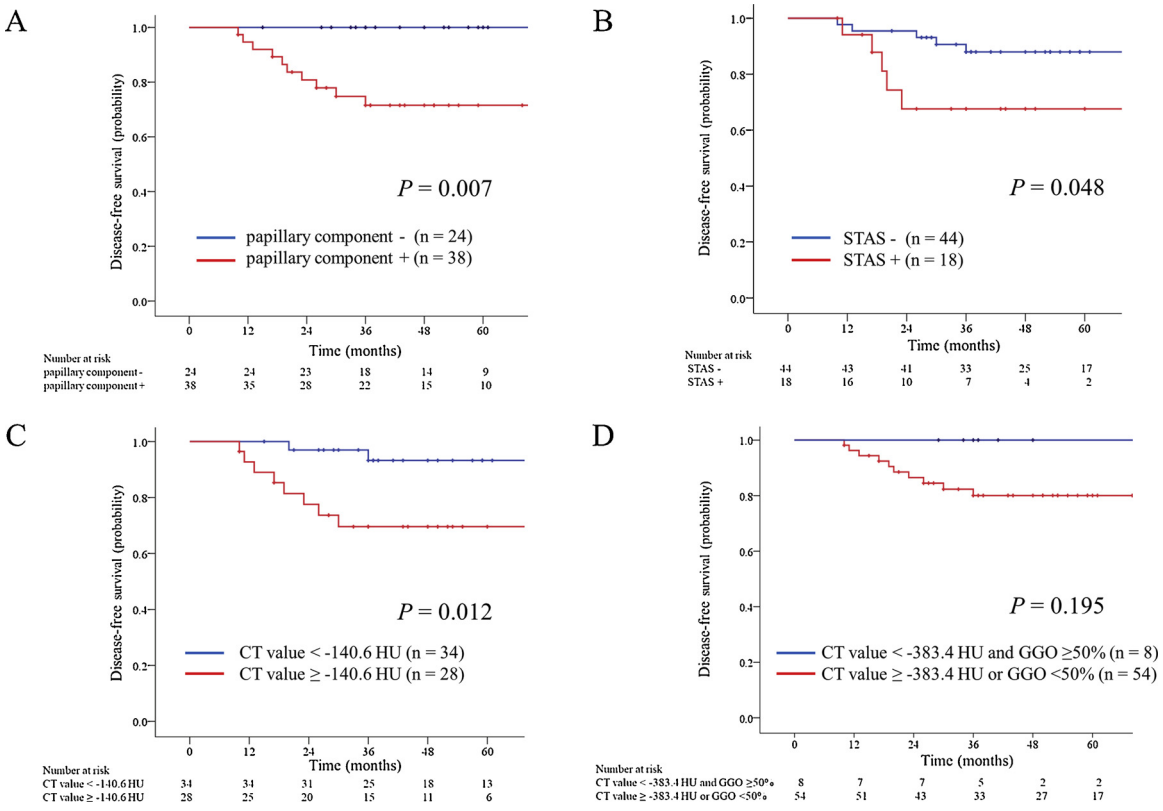

Fig. 5. Kaplan-Meier survival curves for disease-free survival (DFS).
(A) There was a significantly poorer DFS rate in patients with papillary component than without (5-year DFS, 71.5% vs 100%, $p = 0.007$).
(B) There was a significantly poorer DFS rate in patients with STAS-positive lesions than with STAS-negative lesions (5-year DFS, 67.6 vs 87.9%, $p = 0.048$).
(C) There was a significantly poorer DFS rate in patients with CT value > -140.6 HU than CT value < -140.6 HU lesion (5-year DFS, 69.6% vs 93.2%, $p = 0.012$).
(D) No recurrence was observed in the patients in the CT value < -383.4 HU and GGO ≥ 50% group although there were no significant differences between in the CT value < -383.4 HU and GGO ≥ 50% group and CT value ≥ -383.4 HU or GGO < 50% group (5-year DFS, 100% vs 80.0%, $p = 0.195$).

are considered to have a good prognosis with a high proportion of GGO may actually have occult histological nodal involvement and a poor prognosis. In the present study, a small adenocarcinoma appearing as a pure heterogeneous GGO lesion in which a papillary component was observed in a portion associated with a high CT value metastasized to bilateral lungs 3 years after surgery, and the correlation between GGO and lepidic pattern ratios was not very strong. The GGO component of seven (53.0%) pure GGO lesions corresponded to non-lepidic invasive components such as papillary, acinar, solid, and colloid components. These results were consistent with those of previous reports that stated that GGO does not always correspond to lepidic components [8–13]. Prior reports demonstrated that the papillary and acinar subtypes of non-lepidic invasive adenocarcinoma accounted for 5.5–52.2% and 1.8–45.0% of pure GGO lesions, respectively [8–13]. The present results also demonstrated that it is not unusual for GGO to correspond to invasive components other than lepidic components. Moon et al. evaluated the histological components in pure GGO lesions in the same manner as done in this study, and found only lepidic, papillary, and acinar components [10]. Our study adds to previous knowledge that GGO corresponds not only to acinar and papillary components, but also to other invasive components such as solid and colloid components.

In this study, we measured the occupancy ratio of each component (lepidic, papillary, acinar, solid, micropapillary, pattern of variants, fibrosis, necrosis, pleural thickening, inflammation, edema, cavities, vessels, and bronchi) in the whole lesion area, and found that 78.1% of the lesions had more than two histological components, and lesions consisted of at most five components. We also demonstrated that adenocarcinoma of the lung was composed of a variety of components, even within small lesions. The present results are comparable with those of a previous report [2] that demonstrated histological diversity in > 80% of lung adenocarcinomas. Few reports of the histological components within tumors being divided finely and aggregated as done in this study have been reported.

Predominant histological subtypes are significantly associated with prognosis [19–21]. Moreover, minor components may also affect prognosis. Recently, several studies reported that even minor proportions of solid or micropapillary components are associated with worse outcomes [22–25]. The histological criteria for invasive components are any histologic subtype other than lepidic. The identification of non-lepidic invasive components, particularly solid and micropapillary components, could help better predict prognosis. We found that invasive components such as papillary components were observed at a high frequency (60.9%) and solid/micropapillary components were seen in 23.4%/6.3% of tumors. Because papillary component was negative prognostic factors, it is better to consider not only predominant subtypes but also minor components in the same lesions.

STAS is also an important factor when considering postoperative prognosis and selecting a surgical strategy. STAS has newly been reported as a pattern of tumor invasion that spreads within air spaces beyond the edge of the main tumor. Previous studies reported that STAS was a risk factor for recurrence and a poor prognostic factor in adenocarcinomas [15,26–28], in this study also, patients with STAS-positive lesions showed a significantly poorer DFS rate. Several studies reported that pure solid lesions on CT were significantly associated with the presence of STAS [29,30]. However, in the present study, STAS was also observed in one case among pure GGO lesions, and STAS-positive lesion revealed significantly higher CT values.

Simultaneously, our study showed that the CT value of pure GGO lesions is useful for predicting the presence of non-lepidic invasive components. Adenocarcinoma frequently progresses stepwise, developing to invasive carcinoma through atypical adenomatous hyperplasia (AAH), adenocarcinoma in situ (AIS), and minimally invasive adenocarcinoma (MIA) [31]. CT findings of early-stage adenocarcinoma are also diverse, reflecting heterogeneous histological components. At early stages, tumors often consist entirely of GGO. As they progress, the GGO becomes heterogeneous. GGO is defined as an opacity that does not obscure the underlying structures or vasculature [3]. This definition is not associated with an objective numerical value, so it is sometimes difficult to distinguish between dense GGO and solid components. Several studies have reported the use of CT values of pure GGO or part solid GGO lesions to differentiate between pathological types such as AAH, AIS, MIA, and invasive adenocarcinoma. Yagi et al. [32] reported that AIS-MIA was associated with significantly lower mean CT values compared to invasive adenocarcinoma, and Tamura et al. [33] reported that AAH-AIS was associated with significantly lower mean CT values compared to MIA-invasive adenocarcinoma. Tamura et al. showed that the mean CT value could better predict invasive adenocarcinoma than the C/T ratio in small (< 2 cm) lung adenocarcinomas [33]. To the best of our knowledge, no studies have examined histological components correlated with GGO using CT values. We have demonstrated that CT values of pure GGO lesions can help accurately predict non-lepidic invasive components that correspond to GGO.

Previous studies have reported intratumor heterogeneity of PD-L1 expression in adenocarcinomas [17,34,35]. Gagné et al. used microarrays to show that PD-L1 expression varied in different areas of the same surgical specimen [17]. Discordant expression of PD-L1 has also been reported between biopsy specimens and corresponding resected specimens [34]. Consistent with previous reports, we revealed a heterogeneous distribution of PD-L1 expression within a single tumor. We also observed variability in PD-L1 expression among the different histological subtypes within a single tumor. Many researchers have reported that PD-L1 expression is significantly higher in solid and micropapillary predominant adenocarcinomas [35–37]. In contrast, few studies have focused on the association between PD-L1 expression and histological components. Gagné et al. used tissue microarrays to show that in five different cores within the same surgical specimen, PD-L1 expression was significantly higher in the solid and micropapillary components and was lower in acinar, papillary, and lepidic components [17]. However, these authors did not evaluate the entire tumor. Herein we evaluated PD-L1 expression in the whole tumor area using a surgical specimen. In our study, PD-L1 expression was observed in all of the solid and papillary components. Our findings of PD-L1 expression in solid components are consistent with those of previous reports; however, the present findings of papillary component PD-L1 expression differ from those of previous reports. We have demonstrated intratumor heterogeneity by analyzing PD-L1 expression in small adenocarcinomas. These results indicate that intratumor heterogeneity might impact the accuracy of prognostic prediction.

For clinical use of this study, we assessed the combination of GGO ratio and highest CT value inside the tumor and examined whether the prognosis could be predicted by the combination of GGO ratio and highest CT value. Although STAS-positive lesions were strongly associated with a high CT value, lesions containing papillary component were not associated with a high CT value. In the study based on the CT value -140.6 HU in STAS, we could not divide patients with recurrence clearly. Therefore, we used -383.4 HU, which is the lowest CT value in the STAS-positive lesion, and we could differentiate patients without recurrences from patients with those clearly.

The present study also had some limitations. First, this study consisted of a relatively small number of lesions. The histological heterogeneity was proved in cases with pure GGO but this study consisted of a relatively small number of pure GGO lesions. Second, CT findings were compared in a single slice of the maximum area, with histological findings observed in a single slice of the maximum split surface, limiting the accuracy of correlation between CT values and histological findings. For lung adenocarcinomas, CT images and histological findings are both diverse within the same tumor, and further examination is needed to accurately compare images with pathological tissues. Third, PD-L1 was expressed in few tumors. Previous studies have shown that the prevalence of PD-L1 expression was statistically higher in patients with more advanced tumors than in those with early-stage disease [36,38]. We believe that this limitation can be overcome in future

studies, in which PD-L1 expression will be evaluated in many large tumors. Based on these findings, we believe that the present results will be helpful in predicting prognosis and improving outcomes.

In conclusion, radiological/pathological diversity and intratumor heterogeneity makes it difficult to predict prognosis of small (≤ 2 cm) adenocarcinomas. GGO can be indicative of invasive components and STAS can be present even in small GGO lesions. The CT values can be helpful for predicting non-lepidic invasive components of pure GGO lesions, STAS, and prognosis. Based on these findings, combined use of GGO ratio and CT value may help predict the prognosis of GGO lesions and allow better selection of surgical procedures.

Disclosure of funding

This study was supported in part by JSPS KAKENHI Grant Number JP 15K10272.

Acknowledgements

Not applicable.

References

[1] M. Hori, T. Matsuda, A. Shibata, et al., Cancer incidence and incidence rates in Japan in 2009: a study of 32 population-based cancer registries for the Monitoring of Cancer incidence in Japan (MCIJ) project, Jpn. J. Clin. Oncol. 45 (2015) 884–891.
[2] W.D. Travis, E. Brambilla, H.K. Muller-Hermelink, C.C. Harris (Eds.), Pathology and Genetics: Tumours of the Lung, Pleura, Thymus and Heart, IARC Press, Lyon, 2004.
[3] D.M. Hansell, A.A. Bankier, H. MacMahon, et al., Radiology. Fleischner Society: Glossary of Terms for Thoracic Imaging 24 (2008), pp. 697–722.
[4] W.D. Travis, E. Brambilla, M. Noguchi, et al., International Association for the Study of Lung Cancer/American Thoracic Society/European Respiratory Society international multidisciplinary classification of lung adenocarcinoma, J. Thorac. Oncol. 6 (2011) 244–285.
[5] M. Noguchi, A. Morikawa, M. Kawasaki, et al., Small adenocarcinoma of the lung. Histologic characteristics and prognosis, Cancer 75 (1995) 2844–2852.
[6] M. Okada, T. Koike, M. Higashiyama, et al., Radical sublobar resection for small-sized non-small cell lung cancer: a multicenter study, J. Thorac. Cardiovasc. Surg. 132 (2006) 769–775.
[7] T. Koike, T. Koike, S. Sato, et al., Lobectomy and limited resection in small-sized peripheral non-small cell lung cancer, J. Thorac. Dis. 8 (2016) 3265–3274.
[8] J. Ichinose, T. Kohno, S. Fujimori, et al., Invasiveness and malignant potential of pulmonary lesions presenting as pure ground-glass opacities, Ann. Thorac. Cardiovasc. Surg. 20 (2014) 347–352.
[9] H.J. Lim, S. Ahn, K.S. Lee, et al., Persistent pure ground-glass opacity lung nodules $\geq$ 10 mm in diameter at CT scan: histopathologic comparisons and prognostic implications, Chest 144 (2013) 1291–1299.
[10] Y. Moon, K.Y. Lee, J.K. Park, The prognosis of invasive adenocarcinoma presenting as ground-glass opacity on chest computed tomography after sublobar resection, J. Thorac. Dis. 9 (2017) 3782–3792.
[11] H.J. Sim, S.H. Choi, E.J. Chae, et al., Surgical management of pulmonary adenocarcinoma presenting as a pure ground-glass nodule, Eur. J. Cardiothorac. Surg. 46 (2014) 632–636.
[12] B. Chang, J.H. Hwang, Y.H. Choi, et al., Natural history of pure ground-glass opacity lung nodules detected by low-dose CT scan, Chest 143 (2013) 172–178.
[13] C.W. Duann, J.J. Hung, P.K. Hsu, et al., Surgical outcomes in lung cancer presenting as ground-glass opacities of 3 cm or less: a review of 5 years' experience, J. Chin. Med. Assoc. 76 (2013) 693–697.
[14] W.D. Travis, E. Brambilla, A.P. Burke, A. Marx, A.G. Nicholson (Eds.), WHO Classification of Tumours of the Lung, Pleura, Thymus and Heart, 4th ed., IRAC Press, Lyon, 2015.
[15] K. Kadota, J. Nitadori, C.S. Sima, et al., Tumor spread through air spaces is an important pattern of invasion and impacts the frequency and location of recurrences after limited resection for small stage I lung adenocarcinomas, J. Thorac. Oncol. 10 (2015) 806–814.
[16] T. Koike, T. Koike, Y. Yamato, et al., Predictive risk factors for mediastinal lymph node metastasis in clinical stage IA non-small-cell lung cancer patients, J. Thorac. Oncol. 7 (2012) 1246–1251.
[17] A. Gagné, W. Enlow, M.A. Pigeon, et al., Comprehensive assessment of PD-L1 staining heterogeneity in pulmonary adenocarcinomas using tissue microarrays: impact of the architecture pattern and the number of cores, Am. J. Surg. Pathol. 42 (2018) 687–694.
[18] K. Suzuki, T. Koike, T. Asakawa, et al., A prospective radiological study of thin-section computed tomography to predict pathological noninvasiveness in peripheral clinical IA lung cancer (Japan Clinical Oncology Group 0201), J. Thorac. Oncol. 6 (2011) 751–756.
[19] A. Yoshizawa, N. Motoi, G.J. Riely, et al., Impact of proposed IASLC/ATS/ERS classification of lung adenocarcinoma: prognostic subgroups and implications for further revision of staging based on analysis of 514 stage I cases, Mod. Pathol. 24 (2011) 653–664.
[20] P.A. Russell, Z. Wainer, G.M. Wright, et al., Does lung adenocarcinoma subtype predict patient survival?: a clinicopathologic study based on the new International Association for the Study of Lung Cancer/American Thoracic Society/European Respiratory Society international multidisciplinary lung adenocarcinoma classification, J. Thorac. Oncol. 6 (2011) 1496–1504.
[21] A. Yoshizawa, S. Sumiyoshi, M. Sonobe, et al., Validation of the IASLC/ATS/ERS lung adenocarcinoma classification for prognosis and association with EGFR and KRAS gene mutations: analysis of 440 Japanese patients, J. Thorac. Oncol. 8 (2013) 52–61.
[22] N. Yanagawa, S. Shiono, M. Abiko, et al., The clinical impact of solid and micropapillary patterns in resected lung adenocarcinoma, J. Thorac. Oncol. 11 (2016) 1976–1983.
[23] T. Chen, J. Luo, H. Gu, et al., Impact of solid minor histologic subtype in post-surgical prognosis of stage I lung adenocarcinoma, Ann. Thorac. Surg. 105 (2018) 302–308.
[24] Y. Zhang, R. Wang, D. Cai, et al., A comprehensive investigation of molecular features and prognosis of lung adenocarcinoma with micropapillary component, J. Thorac. Oncol. 9 (2014) 1772–1778.
[25] J. Nitadori, A.J. Bograd, K. Kadota, et al., Impact of micropapillary histologic subtype in selecting limited resection vs lobectomy for lung adenocarcinoma of 2cm or smaller, J. Natl. Cancer Inst. 21 (2013) 1212–1220.
[26] H. Uruga, T. Fujii, S. Fujimori, et al., Semiquantitative assessment of tumor spread through air spaces (STAS) in early-stage lung adenocarcinomas, J. Thorac. Oncol. 12 (2017) 1046–1051.
[27] C. Dai, H. Xie, H. Su, et al., Tumor spread thorough air spaces affects the recurrence and overall survival in patients with lung adenocarcinoma &2 to 3cm, J. Thorac. Oncol. 12 (2017) 1052–1060.
[28] K. Masai, H. Sakurai, A. Sukeda, et al., Prognostic impact of margin distance and tumor spread through air spaces in limited resection for primary lung cancer, J. Thorac. Oncol. 12 (2017) 1788–1797.
[29] G. Toyokawa, Y. Yamada, T. Tagawa, et al., Computed tomography features of resected lung adenocarcinomas with spread through air spaces, J. Thorac. Cardiovasc. Surg. 156 (2018) 1670–1676.
[30] S. Shiono, N. Yanagawa, Spread through air spaces is a predictive factor of recurrence and a prognostic factor in stage I lung adenocarcinoma, Interact. Cardiovasc. Thorac. Surg. 23 (2016) 567–572.
[31] M. Noguchi, Stepwise progression of pulmonary adenocarcinoma–clinical and molecular implications, Cancer Metastasis Rev. 29 (2010) 15–21.
[32] T. Yagi, M. Yamazaki, R. Ohashi, et al., HRCT texture analysis for pure or part-solid ground-glass nodules: distinguishability of adenocarcinoma in situ or minimally invasive adenocarcinoma from invasive adenocarcinoma, J. Radiol. 36 (2018) 113–121.
[33] M. Tamura, I. Matsumoto, D. Saito, et al., Mean computed tomography value to predict the tumor invasiveness in clinical stage IA lung cancer, Ann. Thorac. Surg. 104 (2017) 261–266.
[34] M. Ilie, V. Hofman, M. Dietel, et al., Assessment of the PD-L1 status by immunohistochemistry: challenges and perspectives for therapeutic strategies in lung cancer patients, Virchows Arch. 468 (2016) 511–525.
[35] M. Evans, B. O'Sullivan, F. Hughes, et al., The clinicopathological and molecular associations of PD-L1 expression in non-small cell lung Cancer: analysis of a series of 10,005 cases tested with the 22C3 assay, Pathol. Oncol. Res. (2019), https://doi.org/10.1007/s12253-018-0469-6 In press.
[36] H. Uruga, E. Bozkurtlar, T.G. Huynh, et al., Programmed Cell Death Ligand (PD-L1) Expression in Stage II and III Lung Adenocarcinomas and Nodal Metastases, J. Thorac. Oncol. 12 (2017) 458–466.
[37] J. Koh, H. Go, B. Keam, et al., Clinicopathologic analysis of programmed cell death-1 and programmed cell death-ligand 1 and 2 expressions in pulmonary adenocarcinoma: comparison with histology and driver oncogenic alteration status, Mod. Pathol. 28 (2015) 1154–1166.
[38] J.M. Sun, W. Zhou, Y.L. Choi, et al., Prognostic significance of PD-L1 in patients with non-small cell lung Cancer: a large cohort study of surgically resected cases, J. Thorac. Oncol. 11 (2016) 1003–1011.